Development and Validation of a New In-Situ Technique to Measure Total Gaseous Chlorine in Air

Teles C. Furlani[1], RenXi Ye[1], Jordan Stewart[1,2], Leigh R. Crilley[1], Peter M. Edwards[2], Tara F. Kahan[3], Cora J. Young[1*]

[1] Department of Chemistry, York University, Toronto, Canada

[2] Department of Chemistry, University of York, York, UK

[3] Department of Chemistry, University of Saskatchewan, Saskatoon, Canada

*Correspondence to: youngcj@yorku.ca

Abstract

Total gaseous chlorine (TCl$_g$) measurements can improve our understanding of unknown sources of Cl to the atmosphere. Existing techniques for measuring TCl$_g$ have been limited to offline analysis of extracted filters and do not provide suitable temporal information on fast atmospheric process. We describe high time-resolution in-situ measurements of TCl$_g$ by thermolyzing air over a heated platinum (Pt) substrate coupled to a cavity ring-down spectrometer (CRDS). The method relies on the complete decomposition of TCl$_g$ to release Cl atoms that react to form HCl, for which detection by CRDS has previously been shown to be fast and reliable. The method was validated using custom organochlorine permeation devices (PDs) that generated gas-phase dichloromethane (DCM), 1-chlorobutane (CB), and 1,3-dichloropropene (DCP). The optimal conversion temperature and residence time through the high-temperature furnace was 825 °C and 1.5 seconds, respectively. Complete conversion was observed for six organochlorine compounds, including alkyl, allyl, and aryl C-Cl bonds, which are amongst the strongest Cl-containing bonds. The quantitative conversion of these strong C-Cl bonds suggests complete conversion of similar or

26 weaker bonds that characterize all other TCl_g. We applied this technique to both outdoor and indoor

27 environments and found reasonable agreements in ambient background mixing ratios with the sum

28 of expected HCl from known long-lived Cl species. We measured the converted TCl_g in an indoor

29 environment during cleaning activities and observed varying levels of TCl_g comparable to previous

30 studies. The method validated here is capable of measuring in-situ TCl_g and has a broad range of

31 potential applications.

32 **1. Introduction**

33 Chlorine (Cl) containing compounds in the atmosphere can impact air quality, climate, and

34 health (Saiz-Lopez and Von Glasow, 2012; Simpson et al., 2015; Massin et al., 1998; White and

35 Martin, 2010). Gaseous chlorinated compounds are either organic (e.g., dichloromethane,

36 chloroform, and carbon tetrachloride) or inorganic (e.g., Cl_2, HCl, and $ClNO_2$), with inorganic Cl

37 being more reactive under most atmospheric conditions. In this work, total gaseous Cl (TCl_g) refers

38 to all gas-phase Cl-containing species weighted to their Cl content, including both inorganic and

39 organic species. While groups of chlorinated species are often considered based on reactivity

40 considerations (e.g., reactive chlorine, Cl_y), TCl_g includes all molecules that contain one or more

41 Cl atoms:

42 $TCl_g = 4*[CCl_4] + 3*[CHCl_3] + 2*[CH_2Cl_2] + [CH_3Cl] + 2*[Cl_2] + [HOCl] + \ldots\ldots$ E1

43 Impacts on air quality and climate are due to the high reactivity of atomic Cl produced by common

44 atmospheric reactions (e.g., photolysis and oxidation) of Cl-containing compounds (Riedel et al.,

45 2014; Sherwen et al., 2016; Haskins et al., 2018). The Cl cycle is important to atmospheric

46 composition in the stratosphere and troposphere, affecting species including methane, ozone, and

47 particles (both formation and composition), which influence air quality and climate (Solomon,

48 1999; Riedel et al., 2014; Young et al., 2014; Sherwen et al., 2016). High levels of some TCl_g

49   species (e.g., Cl_2 and carbon tetrachloride) are known to be toxic (White and Martin, 2010; Unsal

50   et al., 2021). The implications of many TCl_g species on human health are not well understood for

51   low level exposure for extended periods of time. Potential health impacts of organic chlorinated

52   compounds include hepatotoxicity, nephrotoxicity, and genotoxicity (Unsal et al., 2021;

53   Henschler, 1994). Impacts of inorganic chlorinated species include the chlorination of squalene, a

54   major part of human skin oils, by HOCl (Schwartz-Narbonne et al., 2019); respiratory irritation

55   and airway obstruction by Cl_2 (White and Martin, 2010); and increased incidence of asthma and

56   other chronic respiratory issues following exposure to chloramines (Massin et al., 1998).

57   Sources of Cl to the atmosphere are highly variable and depend on both direct emissions

58   and indirect regional Cl activation chemistry (Finlayson-Pitts, 1993; Raff et al., 2009; Khalil et al.,

59   1999). Direct emissions of TCl_g can come from numerous natural and anthropogenic activities

60   such as, but not limited to, ocean and volcanic emissions, biomass burning, disinfection (i.e.,

61   household cleaning, pool emission, etc), use of solvents and heat transfer coolants, and incineration

62   of chlorinated wastes (Blankenship et al., 1994; Lobert et al., 1999; Keene et al., 1999; Butz et al.,

63   2017; Wong et al., 2017; Fernando et al., 2014). Activation of Cl is another source, occurring when

64   atmospheric processes transform relatively unreactive chloride (Cl^-, such as sea salt, NaCl) into

65   reactive gaseous chlorine (Cl_y), which will contribute to TCl_g. Understanding global levels of TCl_g

66   is difficult due to complex emissions and chemistry. Our best estimates come from modelling

67   studies combined with collaborative efforts to compose policy reports on halogenated substances,

68   such as the World Meteorological Organization (WMO) Scientific Assessment of Stratospheric

69   Ozone Depletion (WMO (World Meteorological Organization), 2018). Mixing ratio estimates of

70   halogenated species from this report are summed from individual measurements (e.g., National

71   Oceanic and Atmospheric Administration (NOAA) and Advanced Global Atmospheric Gases

Experiment (AGAGE)). The WMO report includes flask (captured gas from clean air sectors) and in-situ measurements from field campaigns and routine sampling sites (e.g., CONvective Transport of Active Species in the Tropics (CONTRAST)) (Prinn et al., 2018; Pan et al., 2017; Andrews et al., 2016; Montzka et al., 2021; Adcock et al., 2018). In the most recent WMO report (2018), a decrease of 12.7 ± 0.9 pptv Cl yr^{-1} in total tropospheric Cl was determined for Montreal Protocol-controlled substances (e.g., chlorofluorocarbons (CFCs) and hydrochlorofluorocarbons (HCFCs)). The decrease in Montreal Protocol-controlled emissions has been slightly offset by an increase in relatively short-lived substances (e.g., dichloromethane) that are not controlled by the Montreal Protocol (WMO (World Meteorological Organization), 2018). Despite the emissions of these regulated chlorinated species being relatively well-constrained, new sources for some of these compounds have appeared in the recent past. For example, unexpected increases observed in CFC-11 emissions suggested new unreported production (WMO (World Meteorological Organization), 2018). A new source of chloroform was also recently identified and attributed to halide containing organic matter derived from penguin excrement in the Antarctic tundra (Zhang et al., 2021). Atmospheric levels of TCl_g will additionally be impacted by emission sources that are relatively poorly constrained, including combustion and disinfection. Increasing levels of chlorinated species from known and unknown pathways was observed in a recent ice core study, which estimated an increase of up to 170% of Cl_y (= $BrCl + HCl + Cl + ClO + HOCl + ClNO_3 + ClNO_2 + ClOO + OClO + 2 \cdot Cl_2 + 2 \cdot Cl_2O_2 + ICl$) from preindustrial times to the 1970s could be attributed to mostly anthropogenic sources (Zhai et al., 2021).

Understanding TCl_g source and sink chemistry is not only important for the ambient atmosphere but also for indoor environments. Uncertainty in sources and levels of chemicals, including Cl-containing compounds, indoors is related to heterogeneity in sources and individual

95   indoor environments, and the fact that relatively few studies have focused on indoor chemistry

96   compared to outdoor. The role of chlorinated species on indoor air quality has been investigated

97   in a few studies (Mattila et al., 2020; Wong et al., 2017; Dawe et al., 2019; Giardino and Andelman,

98   1996; Shepherd et al., 1996; Doucette et al., 2018; Nuckols et al., 2005). Most studies have focused

99   on cleaning with Cl-based cleaners, in which HOCl and other inorganic compounds have been

100   observed in the gas phase at high levels (Wong et al., 2017; Wang et al., 2019; Mattila et al., 2020).

101   Some studies have reported the presence of organic chlorinated species such as chloroform and

102   carbon tetrachloride above bleach cleaning solutions indoors (Odabasi, 2008; Odabasi et al., 2014),

103   and chloroform has been observed during water-based cleaning activities, such as showering and

104   clothing washing (Nuckols et al., 2005; Shepherd et al., 1996; Giardino and Andelman, 1996).

105   Constraining the Cl budget is critical to better understanding its contributions to climate,

106   air quality, and human health. Robust total Cl measurements are useful because it is not always

107   feasible to routinely deploy individual measurements of the large number of known Cl-containing

108   compounds (Table S1). As described above, estimates of TCl_g from models and summed

109   measurements have demonstrated gaps in our knowledge. It is therefore essential to have a method

110   capable of measuring true TCl_g to explain discrepancies between model and measured estimates

111   due to unknown species. Measurements of total elemental composition in the condensed phase,

112   including total Cl, have been used for monitoring and managing both known and unknown

113   compounds (Miyake et al., 2007c, a; Yeung et al., 2008; Miyake et al., 2007b; Kannan et al., 1999;

114   Xu et al., 2003; Kawano et al., 2007). However, TCl_g methods have been limited to offline analysis

115   of scrubbed sample gas (e.g., flue); these methods rely on multiple extraction steps and the

116   application of condensed-phase total Cl analyses, such as combustion ion chromatography

117   (Miyake et al., 2007a; Kato et al., 2000) or neutron activation analysis (Berg et al., 1980; Xu et al.,

118   2006, 2007). Because offline techniques suffer from extraction uncertainties and do not have the

119   temporal resolution to effectively probe fast chemistry in the atmosphere, in-situ measurements of

120   total elemental gaseous composition have been developed for several elements (Hardy and Knarr,

121   1982; Veres et al., 2010; Roberts et al., 1998; Maris et al., 2003; Yang and Fleming, 2019). For

122   example, total nitrogen has been measured using Pt-catalyzed thermolysis coupled to online

123   chemiluminescence detection (Stockwell et al., 2018). Using a similar approach, we describe here

124   a method for TCl_g, where catalyzed thermolysis is coupled to a high time-resolution HCl cavity

125   ring-down spectrometer (CRDS). This technique relies on the complete thermolysis of TCl_g, which

126   yields chlorine atoms. These Cl atoms readily form HCl via hydrogen abstraction (R1), in this case

127   from propane (or its thermolysis products) that is supplied in excess.

$$Cl\ (g) + C_3H_8\ (g) \rightarrow HCl\ (g) + C_3H_7\ (g) \hspace{3cm} R1$$
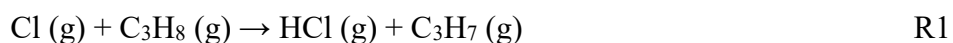
128   The objectives of this paper are to: (i) Develop and validate an instrument capable of in-

129   situ measurement of TCl_g through conversion to HCl and detection by CRDS; and (ii) demonstrate

130   application of the technique to outdoor and indoor TCl_g measurements.

131   **2. Materials and experimental methods**

132   **2.1. Chemicals**

133   Commercially available reagents were purchased from Sigma-Aldrich (Oakville, Ontario,

134   Canada): dichloromethane (DCM, HPLC grade), 1-chlorobutane (CB, 99.5%), cis-1,3-

135   dichloropropene (DCP, 97%), trichlorobenzene (TrCB, 99%), tetrachlorobenzene (TeCB, 98%),

136   pentachlorobenzene (PeCB, 96 %), sodium chloride, and 52 mesh sized platinum catalyst (99.9

137   %). Toluene (HPLC grade) was purchased from BDH VWR (Mississauga, Ontario, Canada).

138   Nitrogen (grade 4.8) and propane (C_3H_8, 12.7% in nitrogen, v/v) gas was from Praxair (Toronto,

139   Ontario, Canada). Experiments used deionized water generated by a Barnstead Infinity Ultrapure

140   Water System (Thermo Fisher Scientific, Waltham, Massachusetts, USA; 18.2 MΩ cm^{-1}). A

permeation device (PD) described previously was used to generate gaseous HCl (Furlani et al., 2021). Chlorine-free zero air was generated by a custom-made zero-air generator.

2.2. HCl and total chlorine (HCl-TCl) instrument

The main components of the HCl-TCl (Figure 1) are platinum catalyst mesh, a quartz glass flow tube, a split-tube furnace (Protégé Compact, 1100°C max temperature, Thermcraft incorporated, North Carolina, USA), and a CRDS HCl analyzer (Picarro G2108 Hydrogen Chloride Gas Analyzer). The platinum catalyst consisted of ~2 g platinum mesh with a total combined surface area of 134 cm^2. Sample gas was mixed with critical orifice-regulated (Lenox laser, Glen Arm, Maryland, USA, 30 psi; SS-4-VCR-2-50) propane gas (62 ± 6 standard cubic centimetres per minute (sccm)), provided in excess prior to introduction to the furnace to promote (R1). The added propane does not fully thermolyze at temperatures < 650 °C, which can lead to spectral interferences in the CRDS analyzer (Figure S1) and should only be added when temperatures exceed 650°C (Furlani et al., 2021). All lines and fittings were made of perfluoroalkoxy (PFA) unless stated otherwise. The mixing line carrying clean air dilution flows was controlled by a 10 L min^{-1} mass flow controller (MFC, GM50A, MKS instruments, Andover, Massachusetts, USA). The length of the sample gas tubing to the furnace was 0.6 m, and the transfer line between the furnace and CRDS was 0.2 m. The furnace transfer line met an overflow tee when delivering flows greater than the CRDS flowrate of 2 L min^{-1}. The coupled CRDS can capture transient fast HCl formation processes on the timescale of a few minutes, limited by the high adsorption activity of HCl on inlet surfaces (discussed further in Section 3.3). The CRDS collects data at 0.5 Hz. Limits of detection (LODs) for the CRDS were calculated as three times the Allan–Werle deviation in raw signal intensity when overflowing the inlet with zero air directed

163 into the CRDS for ~ 10 h. The 30-sec LOD is 18 pptv and well below expected HCl from TCl_g

164 conversion (Furlani et al., 2021a).
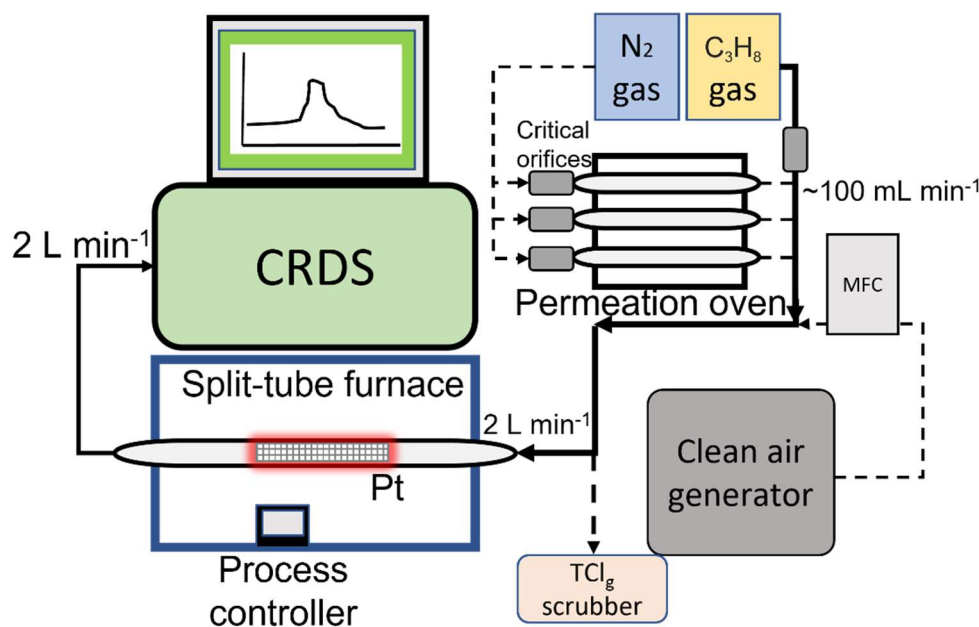
165

166 **Figure 1.** Sampling schematic showing the key components of the HCl-TCl coupled to the CRDS
167 analyzer. Dashed lines indicate parts of the apparatus used only during validation. Not to scale.

2.3. Preparation of organochlorine permeation devices (PDs)

169 Organochlorine PDs were prepared as follows: approximately 200 µL of DCM, CB, or DCP

170 was pipetted into a 50 mm PFA tube (3 mm i.d. with 1 mm thickness), thermally sealed at one end

171 and plugged at the other end with porous polytetrafluoroethylene (PTFE) (13 mm length by 3.17

172 mm o.d.). The polymers allow a consistent mass of standard gas to permeate at a given temperature

173 and pressure. The method for temperature and flow control of the PDs is described in detail in Lao

174 et al. (2020). Briefly, an aluminum block that was temperature-controlled (Omega™; CN 7823,

175 Saint-Eustache, QC, Canada) using a cartridge heater (Omega™; CIR-2081/120V, Saint-Eustache,

176 QC, Canada) housed the PD and was regulated to 30.0 ± 0.1 °C. Dry N_2 gas flowed through a PFA

177 housing tube (1.27 cm o.d.) in the block that contained the PD. Stable flows of carrier gases passed

178 through the housing tube in the oven were achieved using a 50 µm diameter critical orifice (Lenox

179   laser, Glen Arm, Maryland, USA, 30 psi; SS-4-VCR-2-50) and were 120 ± 12, 99 ± 9.9 and 120

180   ± 12 sccm for DCM, CB, and DCP, respectively. Flows were measured using a DryCal Definer

181   220 (Mesa Labs, Lakewood, Colorado, USA). The mass emission rate of each organochlorine from

182   the PDs was quantified gravimetrically over a period of approximately 4 weeks (mass accuracy $\pm$

183   0.001 g). Mass emission rates for each PD were determined as 640 ± 10, 240 ± 40, and 1.20×10^4

184     $\pm 0.02 \times 10^4$ ng min^{-1} (n=3, $\pm 1\sigma$) at 30 °C for DCM, CB, and DCP, respectively.

2.4. HCl-TCl optimization

186   Gas phase standards of DCM, CB, and DCP were used to test the conversion efficiency of

187   chlorinated compounds to form HCl. Bond dissociation energies for carbon-Cl bonds typically

188   range between 310 and 410 kJ mol^{-1} (Tables S1, S2). The split-tube furnace has a process controller

189   capable of increasing or decreasing temperature at a set °C min^{-1}, which allowed us to identify the

190   temperature at which enough energy was provided to break the bonds. By introducing a consistent

191   amount of each of the organochlorines, separately, to the HCl-TCl set over a simple temperature

192   ramping program we could monitor in real-time the conditions necessary to break the bonds by

193   measuring the formation of the resulting HCl. The operating temperature was determined when

194   complete conversion of the measured TCl$_g$ for the tested compounds was sustained at 100%

195   conversion based on PD emission rates.

196   To determine the optimal residence time in the quartz tube with the Pt catalyst, flows of

197   0.6–5.5 L min^{-1} containing DCM sample gas in clean air were tested yielding a range of residence

198   times between 0.5 and 4.5 sec in the furnace. Temperature remained constant at 825 °C throughout

199   the experiment, and a dilution flow of 4.0 L min^{-1} of clean air was added to the sample flow exiting

200   the furnace before introduction to the CRDS.

201   We tested the HCl transmission of the HCl-TCl at 2 mixing ratios (18 and 10 ppbv) using

202   a 12 M HCl PD with zero air dilution flows of 3.5 or 5 L min^{-1} using a 5 L min^{-1} MFC (GM50A,

203   MKS instruments, Andover, Massachusetts, USA). The HCl recovery through the furnace was

204   tested by comparing measured HCl mixing ratios through HCl-TCl to those with the furnace flow

205   tube replaced by a similar length of tubing. A heat gun (Master Varitemp® vt-750c) was used to

206   heat the flow tube entrance to ~80 °C to minimize HCl sorption. We tested the HCl-TCl conversion

207   efficiency for 5 different mixing ratios of three organochlorine PD standards (DCM, CB, and DCP)

208   under three conditions: (1) both Pt catalyst and added propane, (2) only Pt catalyst, and (3) only

209   added propane. Each gas was tested individually under the same conditions; sample gas from PDs

210   was mixed with propane and immediately diluted into clean air using a 10 L min^{-1} MFC. The

211   dilution flows ranged from 2.2–9.0 L min^{-1}. The sampling lines were the same lengths as stated

212   previously. In this experiment, the CRDS flowrate of 2 L min^{-1} was sufficient to give an optimal

213   residence time of 1.5 sec through the HCl-TCl (see Section 3.1). In all experiments the CRDS

214   subsampled through the furnace from the main transfer line and the excess gas was directed

215   outdoors through a waste line containing a carbon trap (Purakol, Purafil, Inc, Doraville, Georgia,

216   USA). We also tested the HCl-TCl conversion efficiency for two different quantities of three

217   chlorobenzenes (TrCB, TeCB, and PeCB). Due to their high boiling points, PDs of these

218   compounds could not be prepared. Instead, small volumes of approximately 1 mM solutions of

219   these compounds dissolved in toluene were directly introduced to the HCl-TCl while it was

220   sampling room air. Room air measurements of TCl_g were consistently >1 ppbv. These were

221   measured before each experiment and did not affect the peak integration described below. With a

222   short piece of tubing used as an inlet, 1 and 2 μL of each compound was injected onto the inner

223   surface of the tubing, which was heated to ~100 °C with a heat gun to facilitate volatilization. The

224 resulting signals were integrated over a time period of 2.5 hours to obtain the total quantity of HCl

225 detected by the CRDS, which was used to calculate conversion efficiency. To account for

226 uncertainties in peak integration, a high and low peak area boundary was determined, with the

227 average peak area taken for each injection. Duplicates of each injected quantity were performed,

228 except for 1 μL TrCB, which was performed in triplicate.

229   To determine if there was any positive bias in the TCl_g, measurement from the conversion

230 of particulate chloride (pCl^-), NaCl aerosols were generated by flowing 2 L min^{-1} of chlorine free

231 zero air through a nebulizer containing a solution of 2% w/w NaCl in deionized water. The aerosol

232 flow was then mixed with 1 L min^{-1} of chlorine free dry zero air to achieve a total flow of 3 L

233 min^{-1}, The HCl-TCl (2 L min^{-1}) then sampled off this main mixing line. Chloride was added after

234 monitoring background zero air levels. After ~3 hours of measuring the converted pCl^-, a PTFE

235 filter (2 μm pore size, 47 mm diameter, TISCH scientific, North Bend, Ohio, USA) was added

236 inline onto the inlet of the HCl-TCl.

237 **2.5. Outdoor air HCl-TCl measurements**

238   Outdoor air sampling was performed between 00:00 on July 7 to 20:00 on July 11, 2022

239 (Eastern daylight time, EDT). The sampling site was the air quality research station located on the

240 roof of the Petrie Science and Engineering building at York University in Toronto, Ontario,

241 Canada (43.7738° N, 79.5071° W, 220 m above sea level). The HCl-TCl was co-located with a

242 Campbell Scientific weather station paired with a cr300 datalogger. All inlet lines and fittings were

243 made of PFA unless stated otherwise. All indoor inlet lines and fittings were kept at room

244 temperature. A mass flow controller (GM50A, MKS instruments, Andover, Massachusetts, USA)

245 regulated a sampling flow of 14.7 L min^{-1} using a diaphragm pump through a 2.4 m sampling inlet

246 (I.D. of 0.375") from outdoors. The outdoor air was pulled through a 2.5 μm particulate matter

247   cut-off URG Teflon Coated Aluminum Cyclone (URG Corporation, Chapel Hill, North Carolina,

248   USA) to remove larger particles and then passed through a PTFE filter (2 μm pore size, 47 mm

249   diameter, TISCH scientific, North Bend, Ohio, USA). The CRDS subsampled 2 L min^{-1} through

250   the furnace off the main inlet line, yielding a total inlet flow of 16.7 L min^{-1}. The apparatus had

251   zero air overflow the inlet 1 hour prior to and after outdoor sampling. The CRDS sample flow

252   passed first through a PTFE filter (2 μm pore size, 47 mm diameter) and then two high efficiency

253   particulate air (HEPA) filters contained within the CRDS outer cavity metal compartment heat-

254   regulated to 45 °C. Instances of flagged instrument errors in the CRDS data during ambient

255   observations were removed as standard practice in quality control procedures. The dataset can be

256   found in Furlani et al., (2022).

2.6.   Indoor air HCl-TCl and HOCl analyzer measurements

258   To test indoor applications of the HCl-TCl, a 1 m^2 area of laboratory floor was cleaned with

259   a commercial spray bottle cleaner (1.84 % sodium hypochlorite w/w) and emissions were

260   compared with an HOCl analyzer. The HOCl analyzer is a commercial instrument designed to

261   quantify gaseous hydrogen peroxide (H$_2$O$_2$) using CRDS (Picarro PI2114 Hydrogen Peroxide

262   Analyzer; Picarro Inc.). The instrument is also sensitive to HOCl due to similar absorbance

263   wavelengths of their first overtone stretches in the near IR. The wavelengths monitored have been

264   altered to selectively detect HOCl. Details on instrument calibration and validation are provided

265   in Stubbs et al. (2022).

266   The distance from the suspended 2 m inlet lines of both instruments to the floor was ~1 m.

267   The flowrate through the furnace and inlet was the 2 L min^{-1} CRDS flowrate. The flowrate for the

268   HOCl analyzer was 1 L min^{-1}. The sectioned off area was cleaned four times, spraying 32 times

269   for each application using the commercial cleaner. Three of these events were measured using the

270 HCl-TCl and HOCl analyzer, while one event was measured using the HCl CRDS only. The

271 dataset can be found in Furlani et al., (2022).

272 **3. Results and Discussion**

273 **3.1.   HCl-TCl temperature and residence time optimization**

274   We validated this method by testing conversion efficiency of organochlorines under different

275 operating parameters and conditions. Testing all TCl_g species is not feasible, but by testing

276 compounds that contain strong Cl-containing bonds, we infer at least equal efficacy of the system

277 in the breakage of relatively weaker Cl-containing bonds (Tables S1 and S2). We selected strong

278 Cl-containing bonds (i.e., alkyl, allyl, and aryl chlorides) and used them as a proxy for compounds

279 containing weaker Cl bonds; therefore, by demonstrating their complete conversion we set

280 precedent for conversion of all TCl_g. The temperature of the furnace is a key factor in

281 accomplishing complete thermolysis, and the minimum temperature of the furnace containing the

282 Pt catalyst to break the C-Cl bonds in DCM was determined. A simple temperature ramping

283 program was used to determine the breakthrough temperature. The temperature was increased at a

284 rate of 2.7 °C min^{-1} starting at 300 °C and ending at 800 °C. The temperature breakthrough was

285 observed when complete conversion of the expected HCl for the tested compounds (based on PD

286 emission rate) was stable after reaching the optimal temperature. It was found to be ~800 °C for

287 the tested organochlorines (Figure S2).

288   Determining the optimal residence time of sample gas in the HCl-TCl is also essential for

289 an optimized TCl_g conversion method. Using a temperature slightly above the observed

290 breakthrough temperature of 800 °C determined above (825 °C), six residence times were tested

291 with DCM, ranging from 0.5 to 4.5 seconds in the HCl-TCl (Figure 2Figure 2). At each residence

292   time the conversion efficiency was determined, where conversion efficiency was calculated as

293   follows:

294   Conversion efficiency $= \frac{\text{Measured TCl}_g}{\text{Expected TCl}_g} \times 100 \%$ E2

295   The optimal residence time was ~1.5 seconds, corresponding to a conversion efficiency of 100.1

296   ± 0.1 %. The uncertainty in conversion efficiency measurements is the variability in the measured

297   HCl signal for 30 minutes after a signal plateau was observed. The reported uncertainty does not

298   include uncertainties in mixing, or turbulence induced surface effects, which we cannot quantify.

299   When residence times were lower (i.e., sample gas traveled more quickly through the system) than

300   1.5 seconds, the conversion efficiencies were lower by 2 – 10 %, the measured HCl signal was

301   more erratic, and it took longer to stabilize. When residence times were higher (i.e., sample gas

302   traveled more slowly through the system) than 1.5 seconds, the conversion efficiencies were

303   comparable (± 2 %), but the measured HCl suffered from longer equilibration times (~30 minutes,

304   more than double the 1.5 residence time) and therefore a slower response time, likely due to

305   increased surface effects of HCl after exiting the furnace. An optimal residence time of 1.5 seconds

306   was selected for all HCl-TCl experiments for its good conversion efficiency and reasonable

307   response time (see Table S3).
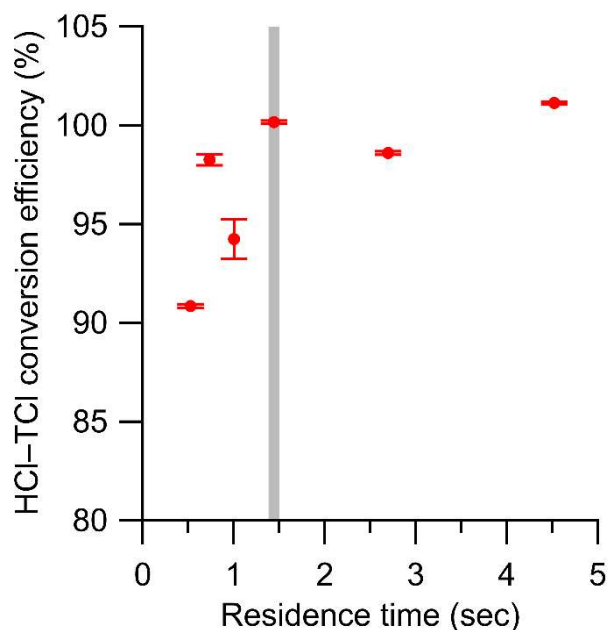
Figure 2. Conversion efficiency of DCM plotted against residence time in the HCl-TCl at 825 °C. Error bars represent the percent relative standard deviation of the measured HCl by the CRDS over ~30 minutes, after signal has plateaued. Grey vertical line denotes the selected residence time. Note that the error bars are represented by the precision of the instrument, and we expect there would be greater experiment-to-experiment variability.

3.2. HCl-TCl conversion efficiency

The efficiency of HCl throughput in the HCl-TCl was tested. Initial tests resulted in transmission efficiencies of 81.2% ± 1.4 (n = 3) and 88.1% (n = 1) for 18 ppbv and 10 ppbv HCl, respectively. At the inlet to the furnace, a small piece of the quartz tube is not heated. We hypothesized that complete transmission of HCl was hindered through sorption to that portion of quartz tube. Repeating the experiment with heat applied led to increased throughput efficiencies of 85.7% (18 ppbv, n = 1) and 93.9% (10 ppbv, n = 1). Therefore, good HCl throughput efficiency was demonstrated overall, with the cause of minor HCl losses identified to be sorption losses to room temperature glass. Conversion of particulate chloride (pCl^-) was observed to take place in the HCl-TCl (Figure S3), but once a filter was introduced the signal returned to background levels. Thus, to capture only gaseous TCl_g from samples that may contain particulate chloride, a

326 particulate filter should be used. Use of a filter could introduce blow on (i.e., partitioning of semi-

327 volatile species) and/or blow off (i.e., processing of particulate chloride) artifacts. We have

328 previously shown that HCl—likely to be the most surface active component of TCl_g—is not greatly

329 impacted by the presence of filters (Furlani et al., 2021), indicating blow on effects are likely

330 minimal. However, the extent to which blow on effects should be considered will depend on the

331 composition of the TCl_g mixture and the temperature. Blow off effects will depend on ambient

332 particulate chloride levels and can be mitigated by regularly changing the filter to prevent

333 significant particulate chloride accumulation.

334   The conversion efficiency of each of the two alkyl chlorine and one allyl chlorine compounds

335 using the HCl-TCl was tested at 5 different mixing ratios. See Table S4 for summary of mixing

336 ratios used; all lower mixing ratios were generated by diluting the highest mixing ratio of each

337 compound by chlorine-free zero air. All three showed good linearity and near 1:1 correlation with

338 the HCl expected to be formed from the PD under standard operating conditions (Figure 3). Due

339 to differences in PD emission rates, the values in Figure 3 are normalized to the highest mixing

340 ratio to visualize comparisons more easily. With both Pt and propane the HCl-TCl conversion was

341 99.6 ± 3.2, 104.8 ± 5.6, and $102.7 \pm 7.8\%$ for DCM, CB, and DCP, respectively (Table 1), as the

342 average conversion efficiency $\pm$ relative standard deviation. From Figure 3 the comparison

343 between expected and measured TCl_g is illustrated by near unity in the orthogonal distance

344 regression slope ($\pm1\sigma$, the error in the regression analysis), and was 0.996 ± 0.012, 1.048 ± 0.060,

345 and 1.027 ± 0.061 for DCM, CB, and DCP, respectively. With only the Pt catalyst, the HCl-TCl

346 conversion was 80.7 ± 0.4, 54.1 ± 1.6, and $54.3 \pm 3.5\%$ for DCM, CB, and DCP, respectively

347 (Figure S4, Table 1). This result indicates the added hydrogen source (propane) is needed to

348 promote R1. Although necessary in this laboratory scenario, some ambient conditions may be rich

349 enough in hydrogen-containing molecules that excess propane is not needed. However, providing

350 propane in excess ensures the presence of an abundance of hydrogen atoms that can be readily

351 abstracted by Cl atoms via R1. When the Pt catalyst was removed, the HCl-TCl conversion was

352 94.4 ± 4.6, 44.2 ± 0.9, and $41.7 \pm 3.4\%$ for DCM, CB, and DCP, respectively (Figure S4, Table

353 1). The observed dependence of the Pt catalyst indicates that a reactive surface is important

354

355
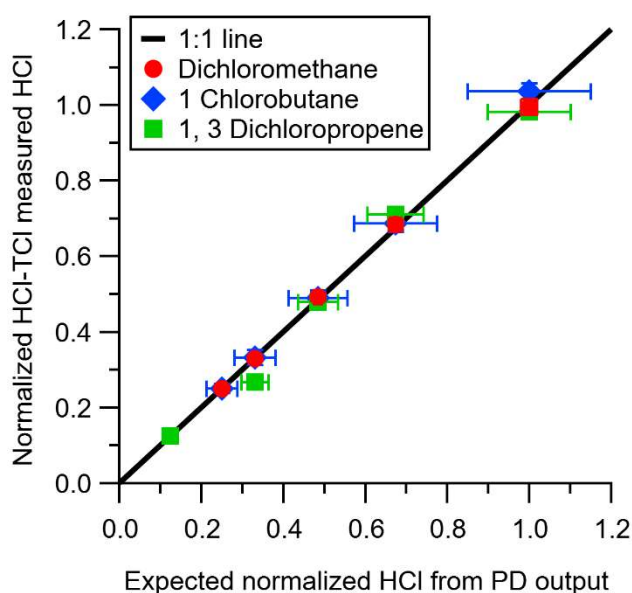
Figure 3. HCl measured by CRDS plotted against the expected HCl from HCl-TCl converted
DCM (red circle), 1-chlorobutane (blue diamond), and 1,3-dichloropropene (green square) under
condition (1). All values are normalized to the highest expected HCl concentration to better
illustrate deviations from unity (black line). Error bars on the y-axis represent 1σ in the HCl signal
over 10 minutes. Error bars on the x-axis represent the uncertainty in the PD used to generate
DCM.

Table 1. Conversion efficiency for tested Cl-containing compounds under different conditions
(both Pt and propane; Pt only; propane only). Note that chlorobenzenes were only tested under
~~final~~ Pt and propane conditions.

Tested TCl$_g$ species	Cl bond dissociation energy (kJ mol^{-1})	Conversion efficiency (%)		
		Pt and propane	Pt only	Propane only
Dichloromethane (DCM)[a]	310	99.6 ± 3.2	80.7 ± 2.4	94.4 ± 6.6
1-Chlorobutane (CB)[a]	410	104.8 ± 5.6	54.1 ± 6.6	44.2 ± 5.9
1, 3-Dichloropropene (DCP)[a]	350	102.7 ± 7.8	54.3 ± 5.2	41.7 ± 5.1

Trichlorobenzene (TrCB)[b]	400	97.0 ± 19.9		
Tetrachlorobenzene (TeCB)[b]	400	90.6 ± 10.3		
Pentachlorobenzene (PeCB)[b]	400	90.2 ± 14.8		

[a]Conversion efficiency was determined from the orthogonal distance regression slope and ± σ and propagated error from individual permeation devices.
[b]Conversion efficiency was determined directly by the quantity (mol) of HCl measured from liquid injections of 1 mM standards. The error represents ±σ of measurements for n = 5 (TrCB) or n = 4 (TeCB, PeCB) injections.

to achieve complete thermolysis at 825 °C. The relatively higher conversion for DCM in the absence of the Pt catalyst or hydrogen source may be attributed to its lower bond dissociation energy (310 kJ mol^{-1}) compared to estimated bond dissociation energies for CB and DCP (CB inferred from Table S2 (~410 kJ mol^{-1}), and DCP from tetrachloroethylene (350 kJ mol^{-1} in Table S1)). It is possible that a higher temperature could lead to full conversion of TCl$_g$ in the absence of Pt catalyst; however, that was not explored in this study. To further validate the HCl-TCl, the conversion efficiency of three aryl chlorine compounds were tested under the final operating conditions (i.e., in the presence of both Pt and added propane). The TCl$_g$ measured from the three aryl compounds was unity, within the uncertainty of the measurement (Table 1).

The results for all six compounds show that the HCl-TCl is capable of complete conversion of mono and polychlorinated species on sp^3 and sp^2 carbons using the determined temperature and flow conditions. The complete thermolysis of the strongest C-Cl bond on the primary alkyl chloride (CB) demonstrates the efficacy of the HCl-TCl. Breaking these relatively strong C-Cl bonds, with consistent conversion efficiency across alkyl, allyl, and aryl C-Cl bonds, is a good proof of concept for complete conversion of all bonds of similar or weaker bond energies that characterize all other TCl$_g$. To practically validate the HCl-TCl under real-world conditions with atmospherically relevant TCl$_g$ mixtures and mixing ratios we also deployed and configured the system to measure outdoor and indoor air.

3.3. Performance metrics of HCl-TCl

Using a flow of zero air through the HCl-TCl, method limits of detection (LODs) were calculated as three times the Allan-Werle deviation (Figure 4) when overflowing a 20 cm inlet (3.17 mm i.d.) with zero air for one hour. The LODs determined in the measurements for 2 second, 1 minute, 5 minute, and 1 hour integration times were 73, 15, 10, and 8 pptv, respectively. The response time of the instrument was assessed during experiments with DCM, CB, and CP. The time for the signal to decay after removal of the PDs was determined to 37 % (1/e) and 90 % (t_{90}) of the maximum signal. The maximum time to achieve 1/e was 23 seconds, while the maximum time to achieve t_{90} was 189 seconds (Table S3). These are comparable to the response times for the HCl CRDS instrument itself (Furlani et al., 2021), suggesting the addition of the inlet furnace has a modest impact on the residence time. Given the high mixing ratios used to test the response times, we argue that under most conditions relevant to indoor and outdoor atmospheric chemistry, a sample integration time of one minute will minimize any time response effects. Data for outdoor and indoor sampling described in Sections 3.4 and 3.5 were therefore averaged to one minute. During all experiments with gaseous reagents, no evidence of catalyst performance degradation was observed.
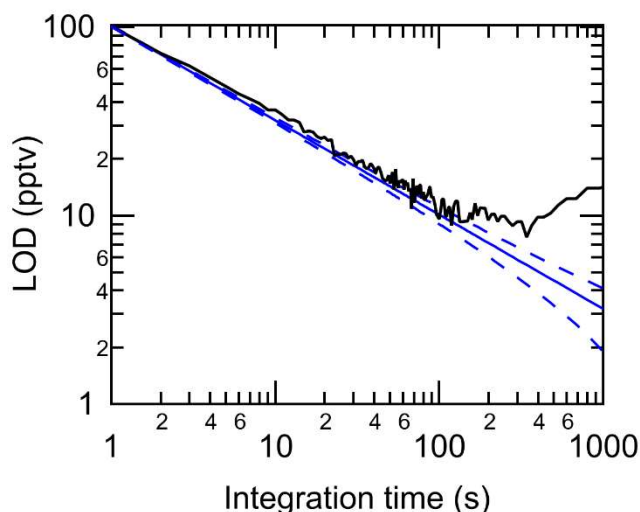
Figure 4. Allan-Werle deviation (3σ) in the HCl-TCl purged with zero-air (black line) shown with the ideal deviation (no drift, solid blue line) and associated error in the deviation (dashed blue line).

3.4. HCl-TCl applications to outdoor air

We deployed the system to measure ambient outdoor air, which we compare to the expected TCl$_g$ range from complete thermolysis of previously measured Cl-containing compounds, estimated to be between 3.3 and 19 ppbv (Table S1). Global background levels of long-lived chlorine-containing species (LLCl$_g$) are well established (WMO (World Meteorological Organization), 2018) and were calculated by equation 3 using data from Table S1:

LLCl$_g$ = 3*[CCl$_3$F] + 2*[CCl$_2$F$_2$] + 4*[CCl$_2$FCCl$_2$F] + 4*[CCl$_3$CClF$_2$] + 3*[CCl$_3$CF$_3$] + 2*[CClF$_2$CClF$_2$] + 2*[CCl$_2$FCF$_3$] + [CClF$_2$CF$_3$] + [CHClF$_2$] + [CH$_2$ClCF$_3$] + 2*[CH$_3$CCl$_2$F] + [CBrClF$_2$] + 4*[CCl$_4$]   E3

A global background for LLCl$_g$ of approximately 2.6 ppbv is expected ((WMO (World Meteorological Organization), 2018), Table S1). The maximum, minimum, and median of observed ambient TCl$_g$ were 536.3, 2.0, and 3.1 ppbv, respectively (Figure 5). Measurements of HCl alone were not made during these periods but reported ranges of HCl mixing ratios for this sampling location from Furlani et al. (2021) and Angelucci et al. (2021) were typically below 110 pptv, with intermittent events up to 600 pptv. The filter present in the inlet was unlikely to have led to artifacts in this measurement. Particulate chloride is negligible in continental summertime environments (Kolesar et al., 2018), indicating blow off artifacts would be minimal. As expected, mMost ambient TCl$_g$ measurements were above the expected mixing ratio of LLCl$_g$. It is possible that semi-volatile chlorinated species could have partitioned to the filter, acting as a blow on effect, and leading to an underestimate of TCl$_g$. However, the warm temperatures during sampling (13 to 31 °C) and high observed TCl$_g$ levels suggest this was not a large effect. There is clear evidence of TCl$_g$ sources beyond LLCl$_g$ at the sampling site, with several plumes of elevated TCl$_g$ intercepted. For example, the maximum TCl$_g$ measurement (536.3 ppbv) was made in a plume just

431 after noon on July 7. Another plume was detected on July 11, with a maximum TCl$_g$ of 42.1 ppbv.

432 Though the purpose of this study was not to determine sources of TCl$_g$, we observed that plumes

433 containing elevated TCl$_g$ arrived from the S-SW of the sampling site, where several facilities that

434 had reported tens to thousands of kg of yearly emissions to air of Cl-containing species are located

435 (Figure S5).

436
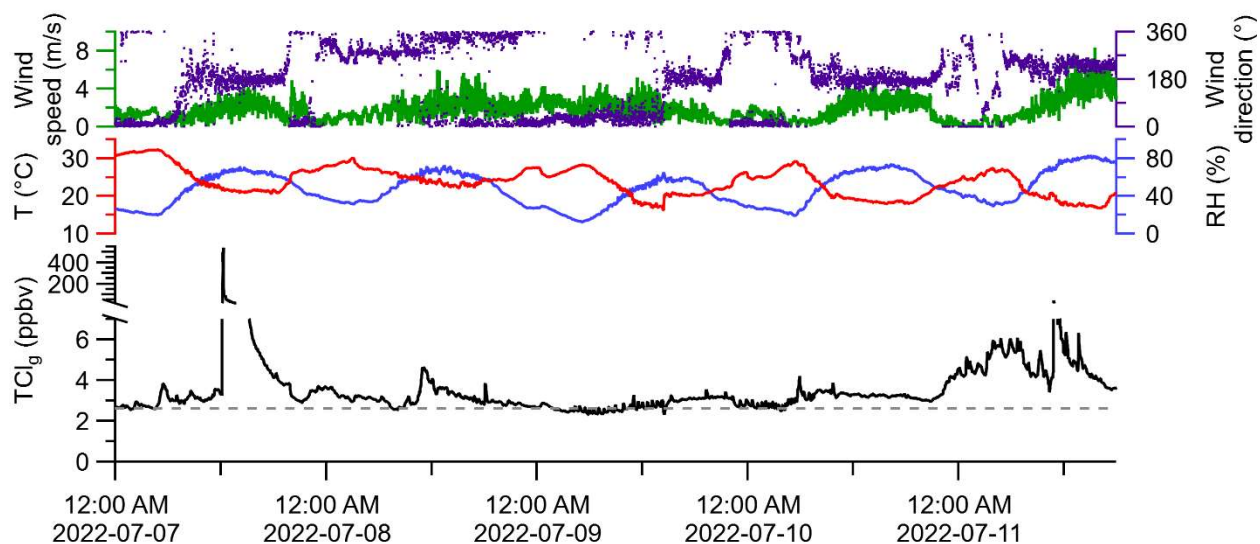
437

438 **Figure 5.** Monitoring meteorological conditions and one-minute averaged TCl$_g$ in outdoor air
439 through HCl-TCl from July 7 to 11, 2022. Grey dashed line represents the background mixing
440 ratio for LLCl$_g$.

441 **3.5. HCl-TCl application to indoor cleaning**

442 We applied a chlorine-based cleaning product four times in a well-lit indoor room and

443 measured TCl$_g$ using the HCl-TCl and HOCl analyzer during three of the cleaning events (Figure

444 6). One cleaning experiment was done without the HCl-TCl and had a maximum of 370 pptv HCl.

445 These levels are comparable to peak HCl levels of ~500 pptv observed from surface application

446 of bleach (Dawe et al., 2019). Consistent with previous speciated measurements (Mattila et al.,

447 2020; Wong et al., 2017), HCl, HOCl, and TCl$_g$ levels increased rapidly over ~5 minutes after the

448 application of the cleaning product. The maximum levels of TCl$_g$ from HCl-TCl during application

449   1, 2, and 3, were 49.2, 80.0, and 69.7 ppbv, respectively. The maximum levels of HOCl from

450   applications 1, 2, and 3, were 19.6, 24.2, and 16.8 ppbv, respectively, corresponding to 24 to 40 %

451   of peak TCl_g and 14 to 22 % of integrated TCl_g. These TCl_g levels were several times higher than

452   most observed in outdoor air (Section 3.4) and were within the range expected from previous

453   experiments (Table S1). The levels of chlorinated species observed during bleaching events is

454   variable, between 15 to 100s of ppbv (Mattila et al., 2020; Odabasi, 2008; Wang et al., 2019; Wong

455   et al., 2017). By comparison, our highest observed mixing ratio was 80 ppbv. Because the

456   multiphase chemical processes involved in bleach application are complex and poorly understood,

457   it is difficult to compare levels between similar studies, given that the underlying ambient

458   conditions can be very different. In addition, physical parameters, such as volume of cleaning

459   solution applied, room size, and ventilation, can all affect observed mixing ratios. For example,

460   studies have observed that gaseous NH_3 partitioning into aqueous bleach can produce large and

461   variable amounts of chloramines, NH_2Cl, $NHCl_2$, and NCl_3 (Mattila et al., 2020; Wong et al.,

462   2017). In our experiments, there was on average 82 ± 4 % of integrated TCl_g that could not be

463   accounted for by the HOCl measurement. Additional chlorinated species that have previously been

464   observed to be emitted from surface bleaching include $ClNO_2$, NH_2Cl, $NHCl_2$, NCl_3, and several

465   chlorinated organics (Odabasi, 2008; Mattila et al., 2020; Wong et al., 2017) which likely also

466   contributed to our measured TCl_g. We observed that TCl_g decayed ~15% faster than the air

467   exchange rate (0.72 h^{-1}), indicating additional chemical loss pathways or surface interactions

468   (Figure S6). We observed a shorter lifetime of HOCl relative to TCl_g, which is consistent with

469   faster decay rates observed for HOCl and similar TCl_g species by Wong et. al., (2017). The HOCl

470   started decreasing after ~300 s had elapsed while the TCl_g levels were still increasing. This

471   suggests that reactions involving HOCl may have led to additional TCl_g species, which has been

472   observed in laboratory studies (Wang et al., 2019).

473   In-situ measurements of TCl_g could provide additional insight into sources of chlorinated

474   species to indoor environments by creating a total inventory from which the contributions of

475   individual measured species can be compared and used to elucidate unknown TCl_g levels and

476   mechanisms in real-time. Furthermore, several chlorinated species that have previously been

477   observed to be emitted from surface bleaching, including Cl_2, HOCl, $ClNO_2$, NH_2Cl, $NHCl_2$, and

478   NCl_3 (Mattila et al., 2020; Wong et al., 2017), have been measured by chemical ionization mass

479   spectrometry (CIMS). Quantifying chlorinated species using CIMS remains challenging due to the

480   required calibrations and difficulty in generating pure gas phase standards. It is therefore desirable

481   to have a technique such as the one proposed in this study that does not require calibrations or

482   knowledge of potential unknown TCl_g species. A combination of the two methods would help

483   constrain the total levels while still observing speciation for key TCl_g species.

484

485
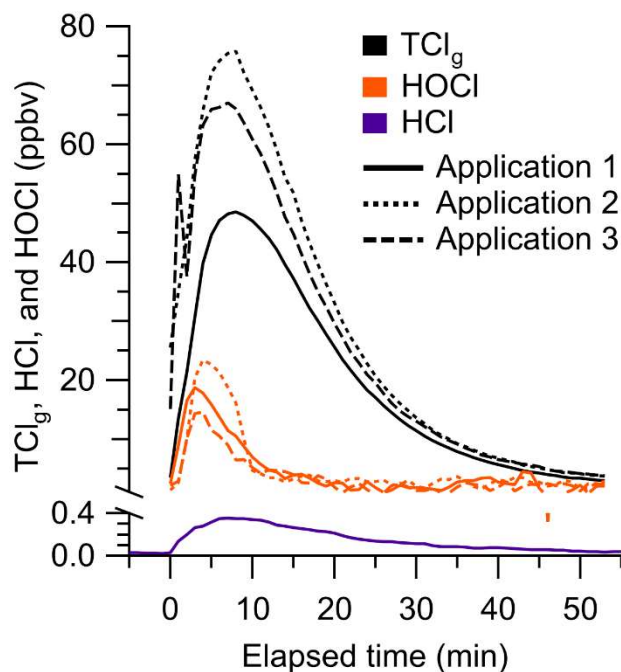
Figure 6. One-minute average HCl (purple), HOCl (orange), and TCl_g (black) observed during cleaning spray events. Mixing ratios were background corrected prior to each cleaning event. Each subsequent application of cleaner is illustrated by a lighter shade for HOCl and TCl_g.

4. Conclusions

In this work we developed, optimized, validated, and applied a method capable of converting TCl_g into gaseous HCl for detection by CRDS. Our TCl_g measurement technique, the HCl-TCl, is composed of a platinum catalyst mesh inside a quartz glass flow tube all contained within a split-tube furnace. The temperature and flow rate were optimized at 825 °C and 1.5 seconds, respectively using DCM. These conditions were validated by the complete conversion of organochlorine compounds with strong C-Cl bonds. The HCl-TCl was used to measure TCl_g outdoors, observing a range of 2.0 to 536.3 ppbv. Levels mostly exceeded the expected background mixing ratio of $LLCl_g$. We also applied the HCl-TCl to an indoor environment during commercial bleach spray cleaning events and observed varying increases in TCl_g (50–80 ppbv), which was in reasonable agreement with levels observed in previous speciated measurements. The agreement of

501 HCl-TCl outdoor and indoor measurements with available bottom-up estimates indicates its

502 efficacy under real-world scenarios. Rapid changes in TCl_g were observed in both outdoor and

503 indoor environments indicating the utility of an in-situ technique to constrain the sources and

504 chemistry of TCl_g, as well as its impact on air quality, climate, and health. We anticipate this

505 approach could be used in several applications, including comparisons to speciated measurements

506 of chlorinated compounds and to further explore Cl reactivity and cycling with respect for indoor

507 and outdoor TCl_g.

Acknowledgements

509 We acknowledge the Sloan Foundation and Natural Sciences Engineering and Research Council

510 of Canada for funding. We thank Melodie Lao and Yashar Iranpour for collecting air exchange

511 rate data, Andrea Angelucci for collecting meteorological data, Dirk Verdoold for the custom

512 quartz tube, and Chris Caputo, John Liggio, Rob McLaren, and Trevor VandenBoer for helpful

513 discussions. PME thanks the European Research Council. TFK is a Canada Research Chair in

514 Environmental Analytical Chemistry. This work was undertaken, in part, thanks to funding from

515 the Canada Research Chairs program.

Author contributions

517 TCF, RY, JS, and LRC collected and analyzed the data. TCF, RY, LRC, and CJY conceived of

518 and designed the experiments with input from PME and TFK. Funding was obtained by TFK and

519 CJY. The manuscript was written by TCF, RY, and CJY with input from all authors.

Data availability

521 Outdoor and indoor datasets can be found in Furlani et al. (2022,

522 https://doi.org/10.20383/103.0649).submitted to Federated Research Data Repository as Furlani,

523 ~~T.C., Ye, R., Stewart, J., Crilley, L.R., Edwards, P.M., Kahan,T.F., Young, C.J. (2022). Outdoor~~

524 ~~and indoor gaseous total chlorine measurement in Toronto Canada. Federated Research Data~~

525 ~~Repository. DOI will be updated when available.~~

Competing interests

527 The authors declare no competing interests.

5. References

529 Adcock, K. E., Reeves, C. E., Gooch, L. J., Leedham Elvidge, E. C., Ashfold, M. J.,
530 Brenninkmeijer, C. A. M., Chou, C., Fraser, P. J., Langenfelds, R. L., Mohd Hanif, N.,
531 O'Doherty, S., Oram, D. E., Ou-Yang, C.-F., Phang, S. M., Samah, A. A., Röckmann, T.,
532 Sturges, W. T., and Laube, J. C.: Continued increase of CFC-113a (CCl3CF3) mixing ratios in
533 the global atmosphere: emissions, occurrence and potential sources, Atmos. Chem. Phys., 18,
534 4737–4751, https://doi.org/10.5194/acp-18-4737-2018, 2018.

535 Andrews, S. J., Carpenter, L. J., Apel, E. C., Atlas, E., Donets, V., Hopkins, J. R., Hornbrook, R.
536 S., Lewis, A. C., Lidster, R. T., Lueb, R., Minaeian, J., Navarro, M., Punjabi, S., Riemer, D., and
537 Schauffler, S.: A comparison of very short lived halocarbon (VSLS) and DMS aircraft
538 measurements in the tropical west Pacific from CAST, ATTREX and CONTRAST, Atmos.
539 Meas. Tech., 9, 5213–5225, https://doi.org/10.5194/amt-9-5213-2016, 2016.

540 Berg, W. W., Crutzen, P. J., Grahek, F. E., Gitlin, S. N., and Sedlacek, W. A.: First
541 measurements of total chlorine and bromine in the lower stratosphere, Geophys Res Lett, 7, 937–
542 940, https://doi.org/https://doi.org/10.1029/GL007i011p00937, 1980.

543 Blankenship, A., Chang, D. P. Y., Jones, A. D., Kelly, P. B., Kennedy, I. M., Matsumura, F.,
544 Pasek, R., and Yang, G.: Toxic combustion by-products from the incineration of chlorinated
545 hydrocarbons and plastics, Chemosphere, 28, 183–196,
546 https://doi.org/https://doi.org/10.1016/0045-6535(94)90212-7, 1994.

547 Butz, A., Dinger, A. S., Bobrowski, N., Kostinek, J., Fieber, L., Fischerkeller, C., Giuffrida, G.
548 B., Hase, F., Klappenbach, F., Kuhn, J., Lübcke, P., Tirpitz, L., and Tu, Q.: Remote sensing of
549 volcanic CO2, HF, HCl, SO2, and BrO in the downwind plume of Mt. Etna, Atmos Meas Tech,
550 10, 1–14, https://doi.org/10.5194/amt-10-1-2017, 2017.

551 Dawe, K. E. R., Furlani, T. C., Kowal, S. F., Kahan, T. F., Vandenboer, T. C., and Young, C. J.:
552 Formation and emission of hydrogen chloride in indoor air, Indoor Air, 70–78,
553 https://doi.org/10.1111/ina.12509, 2019.

554 Doucette, W. J., Wetzel, T. A., Dettenmaier, E., and Gorder, K.: Emission rates of chlorinated
555 volatile organics from new and used consumer products found during vapor intrusion

investigations: Impact on indoor air concentrations, Environ Forensics, 19, 185–190, https://doi.org/10.1080/15275922.2018.1475433, 2018.

Fernando, S., Jobst, K. J., Taguchi, V. Y., Helm, P. A., Reiner, E. J., and McCarry, B. E.: Identification of the Halogenated Compounds Resulting from the 1997 Plastimet Inc. Fire in Hamilton, Ontario, using Comprehensive Two-Dimensional Gas Chromatography and (Ultra)High Resolution Mass Spectrometry, Environ Sci Technol, 48, 10656–10663, https://doi.org/10.1021/es503428j, 2014.

Finlayson-Pitts, B. J.: Chlorine Atoms as a Potential Tropospheric Oxidant in the Marine Boundary Layer, Research on Chemical Intermediates, 19, 235–249, https://doi.org/10.1163/156856793X00091, 1993.

Furlani, T., Ye, R., Stewart, J., Crilley, L., Edwards, P., Kahan, T., and Young, C.: Outdoor and indoor gaseous total chlorine measurement in Toronto Canada [data set], Federated Research Data Repository, https://doi.org/10.20383/103.0649, 2022.

Furlani, T. C., Veres, P. R., Dawe, K. E., Neuman, J. A., Brown, S. S., VandenBoer, T. C., and Young, C. J.: Validation of a new cavity ring-down spectrometer for measuring tropospheric gaseous hydrogen chloride., Atmos Meas Tech, 14, 5859–5871, https://doi.org/https://doi.org/10.5194/amt-2021-105, 2021.

Giardino, N. J. and Andelman, J. B.: Characterization of the emissions of trichloroethylene, chloroform, and 1,2-dibromo-3-chloropropane in a full-size, experimental shower., J Expo Anal Environ Epidemiol, 6, 413–423, 1996.

Hardy, J. E. and Knarr, J. J.: Technique for Measuring the Total Concentration of Gaseous Fixed Nitrogen Species, J Air Pollut Control Assoc, 32, 376–379, https://doi.org/10.1080/00022470.1982.10465412, 1982.

Haskins, J. D., Jaeglé, L., Shah, V., Lee, B. H., Lopez-Hilfiker, F. D., Campuzano-Jost, P., Schroder, J. C., Day, D. A., Guo, H., Sullivan, A. P., Weber, R., Dibb, J., Campos, T., Jimenez, J. L., Brown, S. S., and Thornton, J. A.: Wintertime gas-particle partitioning and speciation of inorganic chlorine in the lower troposphere over the northeast United States and coastal ocean, Journal of Geophysical Research: Atmospheres, 123, 12,897-12,916, https://doi.org/10.1029/2018JD028786, 2018.

Henschler, D.: Toxicity of Chlorinated Organic Compounds: Effects of the Introduction of Chlorine in Organic Molecules, Angewandte Chemie International Edition in English, 33, 1920–1935, https://doi.org/https://doi.org/10.1002/anie.199419201, 1994.

Kannan, K., Kawano, M., Kashima, Y., Matsui, M., and Giesy, J. P.: Extractable Organohalogens (EOX) in Sediment and Biota Collected at an Estuarine Marsh near a Former Chloralkali Facility, Environ Sci Technol, 33, 1004–1008, https://doi.org/10.1021/es9811142, 1999.

Kato, M., Urano, K., and Tasaki, T.: Development of Semi- and Nonvolatile Organic Halogen as a New Hazardous Index of Flue Gas, Environ Sci Technol, 34, 4071–4075, https://doi.org/10.1021/es000881+, 2000.

Kawano, M., Falandysz, J., and Wakimoto, T.: Instrumental neutron activation analysis of extractable organohalogens in the Antarctic Weddell seal (Leptonychotes weddelli), J Radioanal Nucl Chem, 272, 501–504, https://doi.org/10.1007/s10967-007-0611-5, 2007.

Keene, William. C., Khalil, M. A. K., Erickson, David. J., McCulloch, A., Graedel, T. E., Lobert, J. M., Aucott, M. L., Gong, S. L., Harper, D. B., Kleiman, G., Midgley, P., Moore, R. M., Seuzaret, C., Sturges, W. T., Benkovitz, C. M., Koropalov, V., Barrie, L. A., and Li, Y. F.: Composite global emissions of reactive chlorine from anthropogenic and natural sources: Reactive Chlorine Emissions Inventory, Journal of Geophysical Research: Atmospheres, 104, 8429–8440, https://doi.org/10.1029/1998JD100084, 1999.

Khalil, M. A. K., Moore, R. M., Harper, D. B., Lobert, J. M., Erickson, D. J., Koropalov, V., Sturges, W. T., and Keene, W. C.: Natural emissions of chlorine-containing gases: Reactive Chlorine Emissions Inventory, Journal of Geophysical Research: Atmospheres, 104, 8333–8346, https://doi.org/10.1029/1998JD100079, 1999.

Kolesar, K. R., Mattson, C. N., Peterson, P. K., May, N. W., Prendergast, R. K., and Pratt, K. A.: Increases in wintertime PM2.5 sodium and chloride linked to snowfall and road salt application, Atmos Environ, 177, 195–202, https://doi.org/10.1016/j.atmosenv.2018.01.008, 2018.

Lao, M., Crilley, L. R., Salehpoor, L., Furlani, T. C., Bourgeois, I., Neuman, J. A., Rollins, A. W., Veres, P. R., Washenfelder, R. A., Womack, C. C., Young, C. J., and VandenBoer, T. C.: A portable, robust, stable and tunable calibration source for gas-phase nitrous acid (HONO), Atmos Meas Tech, 13, 5873–5890, https://doi.org/10.5194/amt-13-5873-2020, 2020.

Lobert, J. M., Keene, W. C., Logan, J. A., and Yevich, R.: Global chlorine emissions from biomass burning: Reactive Chlorine Emissions Inventory, Journal of Geophysical Research Atmospheres, 104, 8373–8389, https://doi.org/10.1029/1998JD100077, 1999.

Maris, C., Chung, M. Y., Lueb, R., Krischke, U., Meller, R., Fox, M. J., and Paulson, S. E.: Development of instrumentation for simultaneous analysis of total non-methane organic carbon and volatile organic compounds in ambient air, Atmos Environ, 37, 149–158, https://doi.org/https://doi.org/10.1016/S1352-2310(03)00387-X, 2003.

Massin, N., Bohadana, A. B., Wild, P., Héry, M., Toamain, J. P., and Hubert, G.: Respiratory symptoms and bronchial responsiveness in lifeguards exposed to nitrogen trichloride in indoor swimming pools., Occup Environ Med, 55, 258 LP – 263, https://doi.org/10.1136/oem.55.4.258, 1998.

Mattila, J. M., Lakey, P. S. J., Shiraiwa, M., Wang, C., Abbatt, J. P. D., Arata, C., Goldstein, A. H., Ampollini, L., Katz, E. F., DeCarlo, P. F., Zhou, S., Kahan, T. F., Cardoso-Saldaña, F. J., Ruiz, L. H., Abeleira, A., Boedicker, E. K., Vance, M. E., and Farmer, D. K.: Multiphase Chemistry Controls Inorganic Chlorinated and Nitrogenated Compounds in Indoor Air during

Bleach Cleaning, Environ Sci Technol, 54, 1730–1739, https://doi.org/10.1021/acs.est.9b05767, 2020.

Miyake, Y., Kato, M., and Urano, K.: A method for measuring semi- and non-volatile organic halogens by combustion ion chromatography, J Chromatogr A, 1139, 63–69, https://doi.org/https://doi.org/10.1016/j.chroma.2006.10.078, 2007a.

Miyake, Y., Yamashita, N., Rostkowski, P., So, M. K., Taniyasu, S., Lam, P. K. S., and Kannan, K.: Determination of trace levels of total fluorine in water using combustion ion chromatography for fluorine: A mass balance approach to determine individual perfluorinated chemicals in water, J Chromatogr A, 1143, 98–104, https://doi.org/https://doi.org/10.1016/j.chroma.2006.12.071, 2007b.

Miyake, Y., Yamashita, N., So, M. K., Rostkowski, P., Taniyasu, S., Lam, P. K. S., and Kannan, K.: Trace analysis of total fluorine in human blood using combustion ion chromatography for fluorine: A mass balance approach for the determination of known and unknown organofluorine compounds, J Chromatogr A, 1154, 214–221, https://doi.org/https://doi.org/10.1016/j.chroma.2007.03.084, 2007c.

Montzka, S. A., Dutton, G. S., Portmann, R. W., Chipperfield, M. P., Davis, S., Feng, W., Manning, A. J., Ray, E., Rigby, M., Hall, B. D., Siso, C., Nance, J. D., Krummel, P. B., Mühle, J., Young, D., O'Doherty, S., Salameh, P. K., Harth, C. M., Prinn, R. G., Weiss, R. F., Elkins, J. W., Walter-Terrinoni, H., and Theodoridi, C.: A decline in global CFC-11 emissions during 2018−2019, Nature, 590, 428–432, https://doi.org/10.1038/s41586-021-03260-5, 2021.

Nuckols, J. R., Ashley, D. L., Lyu, C., Gordon, S. M., Hinckley, A. F., and Singer, P.: Influence of tap water quality and household water use activities on indoor air and internal dose levels of trihalomethanes, Environ Health Perspect, 113, 863–870, https://doi.org/10.1289/ehp.7141, 2005.

Odabasi, M.: Halogenated Volatile Organic Compounds from the Use of Chlorine-Bleach-Containing Household Products, Environ Sci Technol, 42, 1445–1451, https://doi.org/10.1021/es702355u, 2008.

Odabasi, M., Elbir, T., Dumanoglu, Y., and Sofuoglu, S.: Halogenated volatile organic compounds in chlorine-bleach-containing household products and implications for their use, Atmos Environ, 92, 376–383, https://doi.org/10.1016/j.atmosenv.2014.04.049, 2014.

Pan, L. L., Atlas, E. L., Salawitch, R. J., Honomichl, S. B., Bresch, J. F., Randel, W. J., Apel, E. C., Hornbrook, R. S., Weinheimer, A. J., Anderson, D. C., Andrews, S. J., Baidar, S., Beaton, S. P., Campos, T. L., Carpenter, L. J., Chen, D., Dix, B., Donets, V., Hall, S. R., Hanisco, T. F., Homeyer, C. R., Huey, L. G., Jensen, J. B., Kaser, L., Kinnison, D. E., Koenig, T. K., Lamarque, J.-F., Liu, C., Luo, J., Luo, Z. J., Montzka, D. D., Nicely, J. M., Pierce, R. B., Riemer, D. D., Robinson, T., Romashkin, P., Saiz-Lopez, A., Schauffler, S., Shieh, O., Stell, M. H., Ullmann, K., Vaughan, G., Volkamer, R., and Wolfe, G.: The Convective Transport of Active Species in the Tropics (CONTRAST) Experiment, Bull Am Meteorol Soc, 98, 106–128, https://doi.org/10.1175/BAMS-D-14-00272.1, 2017.

Prinn, R. G., Weiss, R. F., Arduini, J., Arnold, T., DeWitt, H. L., Fraser, P. J., Ganesan, A. L., Gasore, J., Harth, C. M., Hermansen, O., Kim, J., Krummel, P. B., Li, S., Loh, Z. M., Lunder, C. R., Maione, M., Manning, A. J., Miller, B. R., Mitrevski, B., Mühle, J., O'Doherty, S., Park, S., Reimann, S., Rigby, M., Saito, T., Salameh, P. K., Schmidt, R., Simmonds, P. G., Steele, L. P., Vollmer, M. K., Wang, R. H., Yao, B., Yokouchi, Y., Young, D., and Zhou, L.: History of chemically and radiatively important atmospheric gases from the Advanced Global Atmospheric Gases Experiment (AGAGE), Earth Syst. Sci. Data, 10, 985–1018, https://doi.org/10.5194/essd-10-985-2018, 2018.

Raff, J. D., Njegic, B., Chang, W. L., Gordon, M. S., Dabdub, D., Gerber, R. B., and Finlayson-Pitts, B. J.: Chlorine activation indoors and outdoors via surface-mediated reactions of nitrogen oxides with hydrogen chloride, Proceedings of the National Academy of Sciences, 106, 13647 LP – 13654, https://doi.org/10.1073/pnas.0904195106, 2009.

Riedel, T. P., Wolfe, G. M., Danas, K. T., Gilman, J. B., Kuster, W. C., Bon, D. M., Vlasenko, A., Li, S.-M., Williams, E. J., Lerner, B. M., Veres, P. R., Roberts, J. M., Holloway, J. S., Lefer, B., Brown, S. S., and Thornton, J. A.: An MCM modeling study of nitryl chloride ($ClNO_2$) impacts on oxidation, ozone production and nitrogen oxide partitioning in polluted continental outflow, Atmos. Chem. Phys., 14, 3789–3800, https://doi.org/10.5194/acp-14-3789-2014, 2014.

Roberts, J. M., Bertman, S. B., Jobson, T., Niki, H., and Tanner, R.: Measurement of total nonmethane organic carbon (Cy): Development and application at Chebogue Point, Nova Scotia, during the 1993 North Atlantic Regional Experiment campaign, Journal of Geophysical Research: Atmospheres, 103, 13581–13592, https://doi.org/https://doi.org/10.1029/97JD02240, 1998.

Saiz-Lopez, A. and Von Glasow, R.: Reactive halogen chemistry in the troposphere, Chem Soc Rev, 41, 6448–6472, https://doi.org/10.1039/c2cs35208g, 2012.

Schwartz-Narbonne, H., Wang, C., Zhou, S., Abbatt, J. P. D., and Faust, J.: Heterogeneous chlorination of squalene and oleic acid, Environ Sci Technol, 53, 1217–1224, https://doi.org/10.1021/acs.est.8b04248, 2019.

Shepherd, J. L., Corsi, R. L., and Kemp, J.: Chloroform in Indoor Air and Wastewater: The Role of Residential Washing Machines., J Air Waste Manag Assoc, 46, 631–642, https://doi.org/10.1080/10473289.1996.10467497, 1996.

Sherwen, T., Schmidt, J. A., Evans, M. J., Carpenter, L. J., Großmann, K., Eastham, S. D., Jacob, D. J., Dix, B., Koenig, T. K., Sinreich, R., Ortega, I., Volkamer, R., Saiz-Lopez, A., Prados-Roman, C., Mahajan, A. S., and Ordóñez, C.: Global impacts of tropospheric halogens (Cl, Br, I) on oxidants and composition in GEOS-Chem, Atmos. Chem. Phys., 16, 12239–12271, https://doi.org/10.5194/acp-16-12239-2016, 2016.

Simpson, W. R., Brown, S. S., Saiz-Lopez, A., Thornton, J. A., and Von Glasow, R.: Tropospheric Halogen Chemistry: Sources, Cycling, and Impacts, Chem Rev, 115, 4035–4062, https://doi.org/10.1021/cr5006638, 2015.

Solomon, S.: Stratospheric ozone depletion: A review of concepts and history, Reviews of Geophysics, 37, 275–316, https://doi.org/10.1029/1999RG900008, 1999.

Stockwell, C. E., Kupc, A., Witkowski, B., Talukdar, R. K., Liu, Y., Selimovic, V., Zarzana, K. J., Sekimoto, K., Warneke, C., Washenfelder, R. A., Yokelson, R. J., Middlebrook, A. M., and Roberts, J. M.: Characterization of a catalyst-based conversion technique to measure total particulate nitrogen and organic carbon and comparison to a particle mass measurement instrument, Atmos. Meas. Tech., 11, 2749–2768, https://doi.org/10.5194/amt-11-2749-2018, 2018.

Unsal, V., Cicek, M., and Sabancilar, İ.: Toxicity of carbon tetrachloride, free radicals and role of antioxidants, Rev Environ Health, 36, 279–295, https://doi.org/doi:10.1515/reveh-2020-0048, 2021.

Veres, P., Gilman, J. B., Roberts, J. M., Kuster, W. C., Warneke, C., Burling, I. R., and de Gouw, J.: Development and validation of a portable gas phase standard generation and calibration system for volatile organic compounds, Atmos. Meas. Tech., 3, 683–691, https://doi.org/10.5194/amt-3-683-2010, 2010.

Wang, C., Collins, D. B., and Abbatt, J. P. D.: Indoor Illumination of Terpenes and Bleach Emissions Leads to Particle Formation and Growth, Environ Sci Technol, 53, 11792–11800, https://doi.org/10.1021/acs.est.9b04261, 2019.

White, C. W. and Martin, J. G.: Chlorine Gas Inhalation, Proc Am Thorac Soc, 7, 257–263, https://doi.org/10.1513/pats.201001-008SM, 2010.

WMO (World Meteorological Organization): Scientific Assessment of Ozone Depletion: 2018, Report No., Global Ozone Research and Monitoring Project, Geneva, Switzerland, 588 pp. pp., 2018.

Wong, J. P. S., Carslaw, N., Zhao, R., Zhou, S., and Abbatt, J. P. D.: Observations and impacts of bleach washing on indoor chlorine chemistry, Indoor Air, 27, 1082–1090, https://doi.org/10.1111/ina.12402, 2017.

Xu, D., Zhong, W., Deng, L., Chai, Z., and Mao, X.: Levels of Extractable Organohalogens in Pine Needles in China, Environ Sci Technol, 37, 1–6, https://doi.org/10.1021/es025799o, 2003.

Xu, D., Tian, Q., and Chai, Z.: Determination of extractable organohalogens in the atmosphere by instrumental neutron activation analysis, J Radioanal Nucl Chem, 270, 5–8, https://doi.org/10.1007/s10967-006-0302-7, 2006.

Xu, D., Dan, M., Song, Y., Chai, Z., and Zhuang, G.: Instrumental neutron activation analysis of extractable organohalogens in PM2.5 and PM10 in Beijing, China, J Radioanal Nucl Chem, 271, 115–118, https://doi.org/10.1007/s10967-007-0115-3, 2007.

Yang, M. and Fleming, Z. L.: Estimation of atmospheric total organic carbon (TOC) – paving the path towards carbon budget closure, Atmos Chem Phys, 19, 459–471, https://doi.org/10.5194/acp-19-459-2019, 2019.

744 Yeung, L. W. Y., Miyake, Y., Taniyasu, S., Wang, Y., Yu, H., So, M. K., Jiang, G., Wu, Y., Li,
745 J., Giesy, J. P., Yamashita, N., and Lam, P. K. S.: Perfluorinated Compounds and Total and
746 Extractable Organic Fluorine in Human Blood Samples from China, Environ Sci Technol, 42,
747 8140–8145, https://doi.org/10.1021/es800631n, 2008.

748 Young, C. J., Washenfelder, R. A., Edwards, P. M., Parrish, D. D., Gilman, J. B., Kuster, W. C.,
749 Mielke, L. H., Osthoff, H. D., Tsai, C., Pikelnaya, O., Stutz, J., Veres, P. R., Roberts, J. M.,
750 Griffith, S., Dusanter, S., Stevens, P. S., Flynn, J., Grossberg, N., Lefer, B., Holloway, J. S.,
751 Peischl, J., Ryerson, T. B., Atlas, E. L., Blake, D. R., and Brown, S. S.: Chlorine as a primary
752 radical: Evaluation of methods to understand its role in initiation of oxidative cycles, Atmos
753 Chem Phys, 14, 3427–3440, https://doi.org/10.5194/acp-14-3427-2014, 2014.

754 Zhai, S., Wang, X., McConnell, J. R., Geng, L., Cole-Dai, J., Sigl, M., Chellman, N., Sherwen,
755 T., Pound, R., Fujita, K., Hattori, S., Moch, J. M., Zhu, L., Evans, M., Legrand, M., Liu, P.,
756 Pasteris, D., Chan, Y.-C., Murray, L. T., and Alexander, B.: Anthropogenic Impacts on
757 Tropospheric Reactive Chlorine Since the Preindustrial, Geophys Res Lett, 48, e2021GL093808,
758 https://doi.org/https://doi.org/10.1029/2021GL093808, 2021.

759 Zhang, W., Jiao, Y., Zhu, R., Rhew, R. C., Sun, B., and Dai, H.: Chloroform (CHCl3) Emissions
760 From Coastal Antarctic Tundra, Geophys Res Lett, 48, e2021GL093811,
761 https://doi.org/https://doi.org/10.1029/2021GL093811, 2021.

762